

Bound entanglement-assisted prepare-and-measure scenarios

István Márton,¹ Erika Bene,¹ and Tamás Vértesi¹

¹*HUN-REN Institute for Nuclear Research, P.O. Box 51, H-4001 Debrecen, Hungary*

We present a class of linear correlation witnesses that can detect bound entanglement in two-quart Bloch-diagonal states within a three-party prepare-and-measure scenario. We relate the detection power of our witnesses to that of the computable cross norm-realignment (CCNR) criterion. Reliable iterative methods reveal that the separable bound is matched by the classical bound of the correlation witnesses. Several bound entangled states can exceed these bounds, including those with metrological usefulness. In particular, we show that a prominent two-quart bound entangled state with a positive partial transpose (PPT) can be mixed with up to 40% isotropic noise and still be detected as entangled by our prepare-and-measure witness. Furthermore, our witnesses appear to be experimentally practical, requiring only the use of qubit rotations on Alice’s and Bob’s sides and product measurements with binary outcomes on Charlie’s side.

I. INTRODUCTION

The ability to prepare, transform and measure entangled quantum states is of fundamental importance in quantum information science. It underpins not only the development of quantum technologies but also the experimental detection and characterization of entanglement [1, 2]. One of the most puzzling forms of quantum correlations is bound entanglement. This is a form of entanglement that cannot be produced by local operations and classical communication (LOCC). On the other hand, no pure entanglement can be extracted from it by LOCC operations, even if arbitrary copies are available [3]. Nevertheless, it has been shown that bound entanglement is indeed useful and provides a resource for quantum information processing. For instance, it is relevant in quantum many-body systems [4] and has proven valuable in several applications, including quantum key distribution [5], quantum metrology [6–8], activation of quantum resources [9–12], Einstein-Podolsky-Rosen (EPR) steering [13] and Bell nonlocality [14]. More recently, the usefulness of bound entangled states has been demonstrated in prepare-and-measure scenarios [15]. For a recent review of bipartite bound entanglement, see Ref. [16].

In the case of Bell correlations [17], the Bell violations obtained using bipartite bound entangled states with positive partial transpose (PPT) [18] are very small [14, 19, 20]. In contrast, PPT states can generate quantum correlations in prepare-and-measure scenarios, leading to significant violations of classical bounds. This surprising property was recently demonstrated by Carceller and Tavakoli [15] in a three-party prepare-and-measure setup introduced in Ref. [21].

In fact, in dimension-bounded prepare-and-measure scenarios, entanglement enables correlations that are much stronger than those achievable without shared entanglement [22]. An emblematic example is superdense coding [23], where the communication capacity of a single qubit is doubled if the sender and receiver share a two-qubit entangled state. This protocol has recently been reformulated within the prepare-and-measure

framework [24, 25], and a distributed three-party variant has also been proposed [26].

In this work, we introduce a semi-device independent witness for entanglement for 4×4 dimensional three-party prepare-and-measure scenarios that both complements and improves upon the family of witnesses proposed by Carceller and Tavakoli [15] for detecting bound entangled states. While their witness works in prime dimensions and achieves a maximum critical isotropic noise threshold of 28.26% for a 7×7 PPT bound entangled state, our approach is able to detect entanglement in a 4×4 PPT state even when mixed with up to 40% isotropic noise. Moreover, our reliable numerical analysis reveals that, for all the 4×4 states considered, the critical noise threshold for detecting entanglement is identical for both our prepare-and-measure witness and the entanglement witness based on the computable cross norm-realignment (CCNR) criterion [27, 28].

II. SCENARIO

We consider a three-party black-box scenario in which the messages are restricted to dimension four ($d = 4$). Let the three parties, Alice, Bob and Charlie select their inputs x , y , and z , respectively. Each of these inputs is a pair of numbers, where Alice’s input is given by $x = (x_0, x_1) \in \{0, 1, 2, 3\}^2$. Similarly, Bob’s and Charlie’s inputs are $y = (y_0, y_1)$ and $z = (z_0, z_1)$. We define an index $x = 4x_0 + x_1 + 1$, so that x runs from 1 to 16, enumerating the pairs (x_0, x_1) in lexicographic order. Similar indexing is used for Bob’s and Charlie’s input. In our setup, Charlie’s measurement is binary for each input z producing an output $c = \{\pm 1\}$. Fig. 1 provides an illustration of the scenario.

In the entanglement based model, the probability that Charlie obtains outcome c given the inputs x , y , and z is given by

$$P(c|x, y, z) = \text{Tr}(U_x \otimes V_y \rho_{AB} U_x^\dagger \otimes V_y^\dagger M_{c|z}). \quad (1)$$

Here, U_x and V_y are unitary transformations of Alice and Bob, respectively, while $M_{c|z}$ are the elements of Charlie’s positive operator-valued measure (POVM) that add

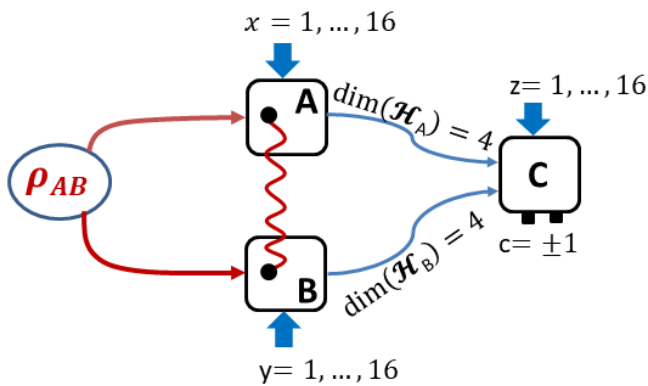


Figure 1. Three-party prepare-and-measure scenario. When entanglement is allowed, Alice and Bob may share any bipartite quantum state ρ_{AB} . They encode their respective inputs $x \in \{1, \dots, 16\}$ and $y \in \{1, \dots, 16\}$ into four-dimensional quantum messages that are sent to Charlie who then decodes these messages with respect to his input $z \in \{1, \dots, 16\}$ and outputs $c = \pm 1$.

up to the identity, $\sum_{c=\pm 1} M_{c|z} = \mathbb{1}$ for every input z . Because the measurement is binary and $P(+1|x, y, z) = 1 - P(-1|x, y, z)$, it is useful to define the expectation value $E_{xyz} = P(+1|x, y, z) - P(-1|x, y, z)$. In the quantum case, it can be expressed as

$$E_{xyz} = \text{Tr}(U_x \otimes V_y \rho_{AB} U_x^\dagger \otimes V_y^\dagger C_z), \quad (2)$$

where C_z is Charlie's dichotomic observable (with eigenvalues ± 1) corresponding to his input z . This captures all the information which is available from a prepare-and-measure experiment with the topology shown in Fig. 1.

We distinguish between two completely different cases based on the property of the quantum state shared by Alice and Bob. In the general case, ρ_{AB} is an arbitrary state acting on a 4×4 dimensional Hilbert space. In contrast, the unentangled or separable case is characterized by states that can be written as

$$\rho_{AB} = \sum_k p_k \rho_k^A \otimes \rho_k^B, \quad (3)$$

where the p_k weights sum up to 1, and ρ_k^A and ρ_k^B are four-dimensional quantum states. A state that cannot be written in this form is entangled. In order to distinguish between entangled and separable states, we make use of linear functionals of the expectation values E_{xyz} in the form of correlation inequalities

$$\sum_{x,y,z} w_{xyz} E_{xyz} \leq Q_{\text{sep}}, \quad (4)$$

with some real coefficients w_{xyz} , which satisfy the tight bound Q_{sep} for all 4×4 separable states (3), unitaries U_x , V_y and observables C_z . Since the witness (4) is linear, it

suffices to optimize over pure product states, and the witness value for separable states can be written as

$$\sum_{x,y,z} w_{xyz} \text{Tr}(\rho_x^A \otimes \rho_y^B C_z), \quad (5)$$

where ρ_x^A and ρ_y^B are representing four-dimensional pure states.

In what follows, we construct a correlation inequality in the form of (4), where the witness coefficients w_{xyz} are tailored to the specific entangled state we wish to detect. To achieve this, we first discuss a class of 4×4 quantum states given by their Bloch decomposition parameters. We then express the witness coefficients in terms of these parameters. Finally, we provide strong numerical evidence that each studied bipartite state violates our correlation inequality if and only if the CCNR criterion detects it as entangled.

III. A CLASS OF BLOCH-DIAGONAL STATES

We consider a class of 4×4 states that can be expressed in a Bloch-diagonal form as

$$\rho_{AB} = \frac{1}{4} \sum_{k=1}^{16} \lambda_k A_k \otimes B_k, \quad (6)$$

where the operators A_k are defined by

$$A_k = \sigma_{k_0} \otimes \sigma_{k_1}, \quad k = (k_0, k_1) \in \{0, 1, 2, 3\}^2, \quad (7)$$

with $\sigma_0 = \mathbb{1}$, $\sigma_1 = X$, $\sigma_2 = Y$, and $\sigma_3 = Z$ being the Pauli matrices. On the other hand, the operator B_k are chosen as $B_k = A_{\mathcal{P}(k)}$, where $\mathcal{P}(k)$ denotes a permutation of the set $\{1, \dots, 16\}$. Note that the sets $\{A_k/2\}_{k=1}^{16}$ and $\{B_k/2\}_{k=1}^{16}$ form orthonormal bases of 4×4 Hermitian operators. That is,

$$\text{Tr} \left(\frac{A_k}{2} \frac{A_l}{2} \right) = \text{Tr} \left(\frac{B_k}{2} \frac{B_l}{2} \right) = \delta_{kl}. \quad (8)$$

In the special case of identity permutation, defined by $\mathcal{P}(k) = k$ for all k , we have $B_k = A_k$. The coefficients λ_k are real (and may take negative values) and are chosen so that ρ_{AB} is a valid quantum state, namely, it must be positive ($\rho_{AB} \geq 0$) and normalized ($\text{Tr}(\rho_{AB}) = 1$). For instance, if $\mathcal{P}(1) = 1$, then $B_1 = A_1$, then we have $\lambda_1 = 1/4$. This kind of Bloch-diagonal states has been discussed in Refs. [29, 30].

Note that any $d \times d$ state $\tilde{\rho}_{AB}$ can be written in its Schmidt form as

$$\tilde{\rho}_{AB} = \sum_k \tilde{\lambda}_k \tilde{A}_k \otimes \tilde{B}_k, \quad (9)$$

where $\{\tilde{A}_k\}_{k=1}^{d^2}$ and $\{\tilde{B}_k\}_{k=1}^{d^2}$ are bases of Hermitian operators satisfying $\text{Tr}(\tilde{A}_k \tilde{A}_l) = \text{Tr}(\tilde{B}_k \tilde{B}_l) = \delta_{kl}$ and the coefficients are given by $\tilde{\lambda}_k = \text{Tr}(\tilde{\rho}_{AB} \tilde{A}_k \otimes \tilde{B}_k)$. Thus, the decomposition (6) above is already in Schmidt form. We now recall the so-called CCNR criterion for entanglement detection of $d \times d$ systems.

Proposition 1. (CCNR criterion [27, 28]) *If a state $\tilde{\rho}_{AB}$ is separable and expressed in the Schmidt form (9), then $CCNR(\tilde{\rho}_{AB}) \equiv \sum_{k=1}^{d^2} |\tilde{\lambda}_k| \leq 1$. If the inequality is violated, the state is entangled.*

Applying Prop. 1 to our family of states, the criterion $\sum_{k=1}^{16} |\lambda_k| > 1$ detects entanglement in the state defined by the Bloch-diagonal form (6). Although this class of states does not contain all possible 4×4 entangled states, as we will see, it does contain a number of states with interesting entanglement properties, including bound entangled states.

IV. PREPARE-AND-MEASURE WITNESSES

We now introduce a family of linear witnesses in the form of correlation inequalities (4) tailored to the class of quantum states (6). Recall that the state in this class is specified by the coefficients λ_k , and the operators $A_k = \sigma_{k_0} \otimes \sigma_{k_1}$ and $B_k = A_{\mathcal{P}(k)}$ for $k = 1, \dots, 16$. Then the witness coefficients w_{xyz} appearing in the correlation inequality (4) are defined by

$$w_{xyz} = \text{sgn}(\lambda_z) \text{Tr}(A_z A_x A_z A_x) \text{Tr}(B_z B_y B_z B_y) \quad (10)$$

for $x, y, z \in \{1, \dots, 16\}$. Here the sign function is defined as

$$\text{sgn}(r) = \begin{cases} -1, & \text{if } r < 0 \\ 0, & \text{if } r = 0 \\ +1, & \text{if } r > 0. \end{cases} \quad (11)$$

Because $|\text{Tr}(A_z A_x A_z A_x)| = |\text{Tr}(B_z B_y B_z B_y)| = 2$ holds for every choice of x, y , and z , each witness coefficient w_{xyz} takes on a value of either 4 or -4 .

In the following subsections, we define a lower bound to the witness value Q_{ent} in the presence of entanglement, and a lower bound to the witness value Q_{sep} when no shared entanglement is present. Based on a reliable iterative method, we conjecture that $Q_{\text{sep}} \leq 4^7$ holds. Numerical evidence supports that this bound is saturated using classical four-dimensional messages, as will be demonstrated in all our examples in Sec. V.

A. Entangled value

We first compute the witness value $Q(\rho_{AB}) = \sum_{xyz} w_{xyz} E_{xyz}$ for the state ρ_{AB} in the Bloch-diagonal form (6), using a special choice of unitary operators and observables. In particular, we set $U_x = A_x = \sigma_{x_0} \otimes \sigma_{x_1}$, $V_y = B_y = A_{\mathcal{P}(y)}$, and $C_z = A_z \otimes B_z$. With these choices, we have the following result.

Proposition 2. *By choosing $U_x = A_x$, $V_y = B_y$ and $C_z = A_z \otimes B_z$ in the expression for the expectation value (2), one obtains*

$$Q(\rho_{AB}) = 4^7 \times CCNR(\rho_{AB}) \quad (12)$$

for the witness value (4), where ρ_{AB} is defined by the operators A_x and B_y in the Bloch-diagonal form (6). This expression provides a lower bound to the maximal value of the witness, Q_{ent} , when shared entanglement is present.

Proof. We write ρ_{AB} using the decomposition (6). Then the expectation value is calculated through the following chain of equalities $E_{xyz} = \sum_k (\lambda_k/4) \text{Tr}(A_k A_x A_z A_x) \text{Tr}(B_k B_y B_z B_y) = (\lambda_z/4) \text{Tr}(A_z A_x A_z A_x) \text{Tr}(B_z B_y B_z B_y)$, where we used that $|\text{Tr}(A_k A_x A_z A_x)| = |\text{Tr}(B_k B_y B_z B_y)| = 2\delta_{k,z}$ holds for any x and y . Then inserting the coefficients (10) in the witness expression, one obtains $Q(\rho_{AB}) = \sum_{xyz} w_{xyz} E_{xyz} = \sum_{xyz} |\lambda_z/4| (\text{Tr}(A_z A_x A_z A_x) \text{Tr}(B_z B_y B_z B_y))^2 = 4^7 \times \sum_z |\lambda_z| = 4^7 \times CCNR(\rho_{AB})$. \square

B. Separable value

With the witness coefficients (10) fixed by the state (6), our next task is to maximize the expression (5) over all product states $\rho_x^A \otimes \rho_y^B$ and measurement observables C_z .

Specifically, a lower bound to the separable value is obtained below by fixing Charlie's observables as $C_z = A_z \otimes B_z$ (for $z = 1 \dots, 16$) and then maximizing over all pure ququart states ρ_x^A and ρ_y^B . Denote this bound by Q_{sep}^M . We next place an upper bound on Q_{sep}^M .

Proposition 3. *The bound satisfies $Q_{\text{sep}}^M \leq 4^7$.*

Proof. Substitute the witness coefficients (10) into the witness expression (4). We then obtain

$$\sum_{xyz} \text{sgn}(\lambda_z) H_{xyz} \text{Tr}(A_z \rho_x^A) \text{Tr}(B_z \rho_y^B), \quad (13)$$

where $H_{xyz} = \text{Tr}((A_z A_x)^2) \text{Tr}((B_z B_y)^2)$. Since $|H_{xyz}| = 16$ and $|\text{sgn}(\lambda_z)| = 1$, we have that the expression (13) is upper bounded by $16 \sum_{xyz} \text{Tr}(A_z \rho_x^A) \text{Tr}(B_z \rho_y^B)$. Applying the Cauchy-Schwarz inequality and using the orthogonality and completeness properties of the observables $\{A_k\}$ and $\{B_k\}$, we arrive at the upper bound $16 \sum_{xy} \sqrt{\sum_z (\text{Tr}(A_z \rho_x^A))^2} \sqrt{\sum_z (\text{Tr}(B_z \rho_y^B))^2} \leq 16 \sum_{x,y} (2 \times 2) = 4^7$. \square

Although $Q_{\text{sep}}^M \leq Q_{\text{sep}}$ by construction, numerical evidence indicates that equality holds in all studied examples (see Sec. V). To reach the bound $Q_{\text{sep}} = 4^7$, we employ a see-saw iterative procedure [31–33] to optimize the witness defined by the coefficients (10). For further details on see-saw methods in the characterization of quantum correlations, see Ref. [34].

A see-saw algorithm. The see-saw iterative method for optimizing a prepare-and-measure witness with fixed coefficients w_{xyz} in Eq. (5) over two-ququart separable states is as follows.

1. Pick a set of random pure states $\{\rho_x^A\}_{x=1}^{16}$ and $\{\rho_y^B\}_{y=1}^{16}$ in Hilbert space of dimension four.
2. Express the witness value as $w = \sum_{z=1}^{16} \text{Tr}(F_z C_z)$, where $F_z = \sum_{xy} w_{xyz} \rho_x^A \otimes \rho_y^B$.
3. Keeping F_z fixed, maximize the objective value w by optimizing over all operators subject to $-\mathbb{1} \leq C_z \leq \mathbb{1}$ for each $z = 1, \dots, 16$. To do so, let $\sum_j c_j^z |\phi_j^z\rangle\langle\phi_j^z|$ be the singular value decomposition of F_z and choose $C_z = \sum_j \text{sgn}(c_j^z) |\phi_j^z\rangle\langle\phi_j^z|$.
4. Rewrite the witness value as $w = \sum_x \text{Tr}(G_x \rho_x^A)$, where $G_x = \sum_{yz} w_{xyz} \text{Tr}_B(\mathbb{1} \otimes \rho_y^B C_z)$. Then, for each x , set $\rho_x^A = |\psi_x\rangle\langle\psi_x|$, where ψ_x is the eigenvector $|\psi_x\rangle$ corresponding to the largest eigenvalue of G_x .
5. Similar to the previous step, update ρ_y^B for fixed ρ_x^A and C_z .
6. Repeat steps 2-5 until convergence of the witness value w in Eq. (5) is reached.

It is important to note that the above see-saw method is heuristic and it can get stuck in a local maximum, so the algorithm is typically repeated several times to ensure global optimality. In our studies, we tested the method on seven different witnesses in Sec. V. By repeating the see-saw scheme, the algorithm has consistently converged to $w = 4^7$. Similar see-saw-type algorithms have been used in various quantum correlation setups, including quantum metrology [7, 12, 35], EPR steering [13], prepare-and-measure scenarios [36, 37], Bell nonlocality [33, 38], and entanglement detection [39, 40], and usually a steady convergence of the algorithm has been observed.

With a slight modification of the above procedure, the witness can also be optimized in the case of a classical model. In this model, instead of quantum messages, Alice and Bob send four-dimensional classical messages to Charlie. The maximum witness value, Q_C can be reproduced by using measurement observables C_z that are diagonal in the computational basis with ± 1 entries. Then the bound Q_C can be computed using the same see-saw procedure, but by initializing the pure states in step 1 to computation basis states, $\{|i_{A,x}\rangle\}_x$ and $\{|i_{B,y}\rangle\}_y$.

In this way we find that the following classical deterministic strategies for Alice and Bob lead to the saturation of $Q_C = 4^7$ in all symmetric cases (i.e., when the operators on both sides are identical, $A_k = B_k$ for $k = (1, \dots, 16)$ in the decomposition given by Eq. (6)). An optimal classical strategy that saturates the bound Q_C turns out to be symmetric as well. Namely, Alice sends the message $m_A = x_1$ (encoded in the basis state $\rho_x^A = |x_1\rangle\langle x_1|$) to Charlie and Bob sends $m_B = y_1$ (encoded in the basis state $\rho_y^B = |y_1\rangle\langle y_1|$) to Charlie, where the inputs are given by $x = (x_0, x_1)$ and $y = (y_0, y_1)$. If Charlie chooses an appropriate decoding strategy, as described in step 3 of the see-saw iterative method, this

procedure will indeed result in $Q_C = 4^7$. Note that the above symmetric deterministic strategy applies to all cases studied except the non-symmetric witnesses specified by the states ρ_{R6}^F and ρ_{R8}^F .

V. EXAMPLES

We now illustrate our findings with seven examples of 4×4 entangled quantum systems. Each entangled state $\rho_{AB}^{(i)}$ with $i = 1, \dots, 7$ has a Bloch decomposition form (6) with coefficients λ_k and operators A_k and B_k as specified in Table I. On the other hand, Table II summarizes our numerical findings, where each row belongs to a different 4×4 state. For each state, we provide the entanglement parameters: \mathcal{N} denotes the entanglement negativity [41], and the CCNR value is due to the computable cross norm or realignment criterion for separability of bipartite states [27, 28].

Note that for each state $\rho_{AB}^{(i)}$ we constructed a witness with the coefficients given in Eq. (10) for which a see-saw procedure consistently yielded $Q_{\text{sep}} = Q_C = 4^7$. Furthermore, we have that $Q(\rho_{AB}) = \text{CCNR}(\rho_{AB}^{(i)}) \times Q_{\text{sep}}$ for each state $i = 1, \dots, 7$ due to Eq. (12). To characterize the state, we define the visibility parameters by considering a mixture of each 4×4 entangled state with an isotropic noise

$$\rho_{AB}^{(i)}(v) = v\rho_{AB}^{(i)} + (1-v)\mathbb{1}_{16}/16. \quad (14)$$

Here, v_{crit} is the critical visibility of the quantum state (14) detected by the prepare-and-measure witness (and, according to our numerical findings, also corresponds to the entanglement threshold detected by the CCNR criterion). Next, v_{metro} denotes the threshold above which the state (14) becomes more useful for quantum metrology than separable states. Then, $v_{\text{loc}}^{(\text{proj})}$ is a lower bound to the visibility threshold below which the state admits a local hidden variable model for projective measurements. Finally, v_{sep} is an (often tight) upper bound on the separability threshold of the state.

Before presenting the states case-by-case, we provide details on the calculation of v_{metro} . Using the numerical method introduced in Ref. [12], we find that the optimal Hamiltonian takes the form

$$H = D_A \otimes \mathbb{1}_4 + \mathbb{1}_4 \otimes D_B, \quad (15)$$

with $D_A = D_B = D$. For all states except ρ_{R8}^F , the matrix is taken as $D = \mathbb{1}_2 \times Z = \text{diag}(+1, -1, +1, -1)$. For ρ_{R8}^F , the optimal choice is $D = Z \times \mathbb{1}_2 = \text{diag}(+1, +1, -1, -1)$. In both cases, D is a local, traceless observable with eigenvalues ± 1 , so that the separability limit for the quantum Fisher information is $\mathcal{F}_{\text{sep}} = 8$. Consequently, v_{metro} is defined as the critical visibility in the mixture (14) for which the maximal quantum Fisher information $\mathcal{F}_Q^{\text{max}}(\rho_{AB}^{(i)}(v))$ reaches 8. Detailed descriptions of all seven quantum states follow.

No.	1	2	3	4	5	6	7
$\lambda_k \setminus \text{State}$	ρ_{ME}	$\rho_{\text{as}}^{\text{W}}$	$\rho_{\text{loc}}^{\text{W}}$	ρ_{R6}^{F}	ρ_{R8}^{F}	ρ_{BPD}	ρ_{Sentsis}
λ_1	1/4	1/4	1/4	1/4	1/4	1/4	1/4
λ_2	1/4	-1/12	-q	0	r_4	1/12	$-s_1$
λ_3	-1/4	-1/12	-q	0	$-r_4$	-1/12	$-s_1$
λ_4	1/4	-1/12	-q	$-r_1$	r_3	-1/12	$-s_1$
λ_5	1/4	-1/12	-q	r_2	r_1	-1/12	$-s_1$
λ_6	1/4	-1/12	-q	r_2	r_4	1/12	$-s_1$
λ_7	-1/4	-1/12	-q	0	$-r_4$	1/12	s_2
λ_8	1/4	-1/12	-q	$-r_2$	$-r_1$	1/12	s_3
λ_9	-1/4	-1/12	-q	0	0	1/12	$-s_1$
λ_{10}	-1/4	-1/12	-q	0	$-r_4$	1/12	s_3
λ_{11}	1/4	-1/12	-q	r_2	$-r_4$	1/12	s_2
λ_{12}	-1/4	-1/12	-q	0	0	-1/12	$-s_1$
λ_{13}	1/4	-1/12	-q	r_3	0	1/12	s_2
λ_{14}	1/4	-1/12	-q	0	$-r_4$	1/12	$-s_1$
λ_{15}	-1/4	-1/12	-q	0	$-r_4$	-1/12	s_3
λ_{16}	1/4	-1/12	-q	r_1	0	1/12	$-s_1$

Table I. **Coefficients of the Bloch-diagonal 4×4 states.** The table lists the coefficients λ_k (with $k = 1, \dots, 16$) for the explicit decomposition of the entangled quantum states under study. The parameters are defined as follows: $q = 19/340$, $r_1 = (\sqrt{2}-1)/4$, $r_2 = (2-\sqrt{2})/4$, $r_3 = r_2 - r_1$, $r_4 = r_2/2$ and $s_1 = 0.0557066$, $s_2 = 0.0142664$, $s_3 = 0.0971467$. Each state ρ_{AB} is defined in formula (6) using the product of Pauli operators $A_k = B_k = \sigma_{k_0} \otimes \sigma_{k_1}$ for $k = 1, \dots, 16$, except in two cases: for the state ρ_{R6}^{F} , the operators are modified by setting $B_{11} = A_6$, $B_6 = A_{11}$, for the state ρ_{R8}^{F} , the modifications are $B_{10} = A_{11}$, $B_{11} = A_{10}$, $B_{14} = A_{15}$, and $B_{15} = A_{14}$.

1. Maximally entangled 4×4 state: The state $\rho_{\text{ME}} = |\Phi_4^+\rangle\langle\Phi_4^+|$ with $|\Phi_4^+\rangle = 1/2 \sum_{k=1}^4 |k\rangle|k\rangle$ has Bloch-decomposition coefficients as given in the first column of Table I. Its CCNR value is $\sum_{k=1}^{16} |\lambda_k| = 4$. When mixed with white noise,

$$\rho_{\text{ME}}(v) = v|\Phi_4^+\rangle\langle\Phi_4^+| + (1-v)\mathbb{1}_{16}/16, \quad (16)$$

the resulting isotropic state is entangled for $v > 0.2$, i.e., $v_{\text{sep}} = 0.2$ (as determined by the PPT criterion [18]), and $v_{\text{crit}} = 0.2$ coincides with this value. Moreover, there exists a local model for projective measurements for $v \leq \sum_{k=2,3,4} 1/(3k) \simeq 0.3611$ [42], which yields $v_{\text{loc}}^{(\text{proj})} \simeq 0.3611$. The state is useful for metrology with the Hamiltonian (15) if $v > (1/32) \times (7 + \sqrt{113}) \simeq 0.5509$ (see the Supp. Mat. in Ref [12]).

2. Antisymmetric 4×4 Werner state: As part of the $d \times d$ Werner family [43], this state is given by

$$\rho_{\text{W}}(p) = pP_{\text{as}}/6 + (1-p)P_{\text{sym}}/10, \quad (17)$$

where $P_{\text{as}} = (\mathbb{1}_4 - V)/2$ and $P_{\text{sym}} = (\mathbb{1}_4 + V)/2$ are projectors on the respective antisymmetric and symmetric spaces, with V being the swap operator, $V = \sum_{ij} |ji\rangle\langle ij|$. For $p = 1$, the state is defined as $\rho_{\text{as}}^{\text{W}} = P_{\text{as}}/6$ and

No.	State	\mathcal{N}	CCNR	v_{crit}	v_{metro}	$v_{\text{loc}}^{(\text{proj})}$	v_{sep}
1	ρ_{ME}	1.5	4	0.2	0.5509	0.3611	0.2
2	$\rho_{\text{as}}^{\text{W}}$	0.25	1.5	0.6	0.8496	0.75	0.2
3	$\rho_{\text{loc}}^{\text{W}}$	0.1471	1.0882	0.8947	-	1	0.2983
4	ρ_{R6}^{F}	0	1.0858	0.8974	0.9183	-	0.7446
5	ρ_{R8}^{F}	0	1.0858	0.8974	0.9183	-	0.7446
6	ρ_{BPD}	0	1.5	0.6	-	-	0.6
7	ρ_{Sentsis}	0	1.0856	0.8976	-	-	0.7814

Table II. **Entanglement and critical noise parameters of the Bloch-diagonal 4×4 states.** Each entangled state $\rho_{\text{AB}}^{(i)}$ (with $i = 1, \dots, 7$) shown in a separate row is expressed in the Bloch-decomposition form (6) with coefficients λ_k and operators A_k and B_k as given in Table I. The subsequent columns list the following parameters: \mathcal{N} denotes the entanglement negativity [41] and CCNR denotes the value obtained from the computable cross norm-realignment criterion [27, 28]. These measures detect entanglement when $\mathcal{N} > 0$ and $\text{CCNR} > 1$, with the maximum values for 4×4 systems given by $\mathcal{N} = 1.5$ and $\text{CCNR} = 4$, respectively. The critical visibility parameters refer to the state $\rho_{\text{AB}}^{(i)}$ mixed with isotropic noise $\rho_{\text{iso}} = \mathbb{1}_{16}/16$. In the prepare-and-measure scenario and in the metrology setup, the corresponding thresholds are denoted by v_{crit} and v_{metro} , respectively. In the Bell scenario, $v_{\text{loc}}^{(\text{proj})}$ denotes a lower bound to the visibility below which the state admits a local model for projective measurements, while v_{sep} in the last column represents an upper bound to the separability threshold of the state.

has a CCNR value of $\sum_{k=1}^{16} |\lambda_k| = 3/2$. When mixed with isotropic noise $(1-v)$, the state remains within the Werner class and is known to be separable only when it is PPT, hence, the state is entangled for $v > 0.2$. It admits a local hidden variable model for projective measurements for $v \leq 3/4$ (Ref. [43]) and it becomes metrologically useful when $v > 0.8496$. However, note that $v_{\text{crit}} = 0.6$, which is much higher than $v_{\text{sep}} = 0.2$. These states exhibit a high degree of symmetry and shareability [44], and can also be used for quantum data hiding [45].

3. 4×4 Werner state with a local hidden variable model: The state is defined as $\rho_{\text{loc}}^{\text{W}} = \rho_{\text{W}}(27/34)$ in Eq. (17). The parameter $p = 27/34$ marks the threshold below which Werner's local hidden variable model applies. Although the mixture (14) is entangled for $v > 0.2983$ (by the PPT criterion [18]) and $v_{\text{crit}} = 0.8947$, the state is not useful for metrology since its maximum quantum Fisher information (with Hamiltonian (15)) is only $\mathcal{F}_Q^{\text{max}} = 5.2271 < 8$.

4. A metrologically useful rank-6 bound entangled state: Denoted by ρ_{R6}^{F} , this state is given in Supp. Mat. of Ref. [7] and is extremal within the set of 4×4 PPT entangled states [46]. Ref. [8] shows that it is local unitarily equivalent to the state defined in Ref. [5], which is part of a family of $2d \times 2d$ states known as private states [5]. The separability threshold of the mixture (14) is $v_{\text{sep}} = 0.7446$ (determined by not having a

2-copy PPT symmetric extension [47], implemented using the QETLAB package [48]). The critical visibility for our prepare-and-measure witness is $v_{\text{crit}} = 0.8974$. The state has $\mathcal{F}_Q^{\text{max}} = 32 - 16\sqrt{2} \simeq 9.3726 > 8$ with the optimal Hamiltonian (15), where $D = \text{diag}(+1, +1, -1, -1)$, making it useful for metrology for $v > 0.9183$. No local hidden variable model is known for this state.

5. A metrologically useful rank-8 bound entangled state: The state $\rho_{R8}^{\mathcal{F}}$ has the same metrological performance as $\rho_{R6}^{\mathcal{F}}$ but differs in rank and is not invariant under partial transposition. Its Bloch-decomposition coefficients are given in Table I. An equivalent state up to local unitary transformations is given in Ref. [8]. The state is part of a $2d \times 2d$ family of states described in Section V of Ref. [8] and is also available in the QUBIT4MATLAB package [49] (see the routine `BES_metro.m`). It has the same separability threshold $v_{\text{sep}} = 0.7446$, prepare-and-measure threshold $v_{\text{crit}} = 0.8974$ and maximum quantum Fisher information $\mathcal{F}_Q^{\text{max}} = 32 - 16\sqrt{2} \simeq 9.3726$ as for the state $\rho_{R6}^{\mathcal{F}}$. In this case, the optimal Hamiltonian (15) is $D = \text{diag}(+1, -1, +1, -1)$, and it becomes useful for metrology when $v > 0.9183$. Again, we are not aware of any local hidden variable model for this state.

6. A 4×4 Bell product diagonal state: Introduced in Ref. [50], the state ρ_{BPD} when mixed with white noise is determined to be entangled (via the CCNR criterion [27, 28]) for $v > 0.6$, corresponding to $v_{\text{sep}} = v_{\text{crit}} = 0.6$. The routine `BES_CCNR4x4.m` in the QUBIT4MATLAB package [49] defines this state. Some other references on the Bell product diagonal state include Refs. [29, 40, 51]. Numerical analysis indicates that this state maximizes the CCNR value (at 1.5) among 4×4 PPT entangled states [40]. A very similar state is provided in Ref. [52] with the same CCNR value. However, we are not aware of any local hidden variable model, and the state is not metrologically useful since $\mathcal{F}_Q^{\text{max}} = 5.3333 < 8$ for any Hamiltonian of the form (15).

7. Sentis et al. state: The state ρ_{Sentis} is defined in Ref. [30] which detects bound entanglement with high statistical significance, making it robust for experimental certification. When mixed with white noise, it is determined to be entangled for $v > 0.7814$ using the Breuer-Hall positive maps [53, 54]. It is not useful metrologically, as $\mathcal{F}_Q^{\text{max}} = 4.8913 < 8$ with any Hamiltonian of the form (15), and is not known to admit a local hidden variable model. The critical visibility of the mixture (14) corresponding to both the CCNR criterion and to the prepare-and-measure setup is $v_{\text{crit}} = 0.8976$.

VI. DISCUSSIONS

We presented a family of linear entanglement witnesses designed for a three-party prepare-and-measure scenario that are capable of detecting entanglement in 4×4 Bloch-diagonal states. These witnesses are tailored to the specific quantum state to be detected. To test their performance, we applied our construction to seven different states, including some that are PPT bound entangled, and added isotropic noise to each state. In every 4×4 case, our tailored prepare-and-measure witness exceeded the separable bound precisely when the CCNR criterion detected that the noisy state was entangled. Although determining the separable bound for these witnesses relied on heuristic methods, our numerical algorithm consistently found that this bound matched the separable bound obtained from the CCNR-based entanglement witness.

Our prepare-and-measure witness, although based on a similar setup, differs from that of Carceller and Tavakoli [15] in several key aspects. While their witness is limited to prime dimensional component spaces and achieves a maximum critical isotropic noise tolerance of 28.26% for 7×7 systems, our witness attains an even higher tolerance of 40% in a 4×4 PPT bound entangled state. Notably, both schemes exhibit noise robustness that exceeds the levels known for Bell nonlocality with bipartite bound entanglement [14, 19, 20], making them both promising for practical implementations. Furthermore, the measurements in both Ref. [15] and this work are separable, with ours being product measurements, which are much easier to implement than entangled measurements. Another advantage of our scheme is that it requires only two-outcome measurements to reveal the role of bound entanglement.

Finally, the strong connection we explored between our prepare-and-measure witness and the CCNR witness in the specific case of 4×4 Bloch-diagonal states raises an intriguing question: Can this link be extended to more general 4×4 states or even to states with local dimensions beyond four?

Acknowledgments

We acknowledge the support of the EU (CHIST-ERA MoDIC) and the National Research, Development and Innovation Office NKFIH (No. 2023-1.2.1-ERA_NET-2023-00009 and No. K145927).

[1] O. Gühne and G. Tóth, Entanglement detection, *Phys. Rep.* **474**, 1 (2009).
 [2] R. Horodecki, P. Horodecki, M. Horodecki, and K. Horodecki, Quantum entanglement, *Rev. Mod. Phys.* **81**, 865 (2009).

[3] M. Horodecki, P. Horodecki, and R. Horodecki, Mixed-state entanglement and distillation: Is there a “bound” entanglement in nature?, *Phys. Rev. Lett.* **80**, 5239 (1998).
 [4] G. Tóth, C. Knapp, O. Gühne, and H. J. Briegel, Optimal spin squeezing inequalities detect bound entanglement in

- spin models, *Phys. Rev. Lett.* **99**, 250405 (2007).
- [5] K. Horodecki, M. Horodecki, P. Horodecki, and J. Oppenheim, Secure key from bound entanglement, *Phys. Rev. Lett.* **94**, 160502 (2005).
- [6] L. Czekaj, A. Przysiężna, M. Horodecki, and P. Horodecki, Quantum metrology: Heisenberg limit with bound entanglement, *Phys. Rev. A* **92**, 062303 (2015).
- [7] G. Tóth and T. Vértesi, Quantum states with a positive partial transpose are useful for metrology, *Phys. Rev. Lett.* **120**, 020506 (2018).
- [8] K. F. Pál, G. Tóth, E. Bene, and T. Vértesi, Bound entangled singlet-like states for quantum metrology, *Phys. Rev. Res.* **3**, 023101 (2021).
- [9] P. Horodecki, M. Horodecki, and R. Horodecki, Bound entanglement can be activated, *Phys. Rev. Lett.* **82**, 1056 (1999).
- [10] L. Masanes, All bipartite entangled states are useful for information processing, *Phys. Rev. Lett.* **96**, 150501 (2006).
- [11] L. Tendick, H. Kampermann, and D. Bruß, Activation of nonlocality in bound entanglement, *Phys. Rev. Lett.* **124**, 050401 (2020).
- [12] G. Tóth, T. Vértesi, P. Horodecki, and R. Horodecki, Activating hidden metrological usefulness, *Phys. Rev. Lett.* **125**, 020402 (2020).
- [13] T. Moroder, O. Gittsovich, M. Huber, and O. Gühne, Steering bound entangled states: A counterexample to the stronger Peres conjecture, *Phys. Rev. Lett.* **113**, 050404 (2014).
- [14] T. Vértesi and N. Brunner, Disproving the Peres conjecture by showing Bell nonlocality from bound entanglement, *Nature Communications* **5**, 10.1038/ncomms6297 (2014).
- [15] C. R. i Carceller and A. Tavakoli, Bound entangled states are useful in prepare-and-measure scenarios (2024), arXiv:2410.15388 [quant-ph].
- [16] B. C. Hiesmayr, C. Popp, and T. C. Sutter, Bipartite bound entanglement (2024), arXiv:2406.13491 [quant-ph].
- [17] N. Brunner, D. Cavalcanti, S. Pironio, V. Scarani, and S. Wehner, Bell nonlocality, *Rev. Mod. Phys.* **86**, 419 (2014).
- [18] A. Peres, Separability criterion for density matrices, *Phys. Rev. Lett.* **77**, 1413 (1996).
- [19] S. Yu and C. H. Oh, Family of nonlocal bound entangled states, *Phys. Rev. A* **95**, 032111 (2017).
- [20] K. F. Pál and T. Vértesi, Family of Bell inequalities violated by higher-dimensional bound entangled states, *Phys. Rev. A* **96**, 022123 (2017).
- [21] P. Bakhshinezhad, M. Mehboudi, C. R. i Carceller, and A. Tavakoli, Scalable entanglement certification via quantum communication, *PRX Quantum* **5**, 020319 (2024).
- [22] A. Tavakoli, J. Pauwels, E. Woodhead, and S. Pironio, Correlations in entanglement-assisted prepare-and-measure scenarios, *PRX Quantum* **2**, 040357 (2021).
- [23] C. H. Bennett and S. J. Wiesner, Communication via one- and two-particle operators on Einstein-Podolsky-Rosen states, *Phys. Rev. Lett.* **69**, 2881 (1992).
- [24] G. Moreno, R. Nery, C. de Gois, R. Rabelo, and R. Chaves, Semi-device-independent certification of entanglement in superdense coding, *Phys. Rev. A* **103**, 022426 (2021).
- [25] A. Tavakoli, A. A. Abbott, M.-O. Renou, N. Gisin, and N. Brunner, Semi-device-independent characterization of multipartite entanglement of states and measurements, *Phys. Rev. A* **98**, 052333 (2018).
- [26] J. Bowles, N. Brunner, and M. Pawłowski, Testing dimension and nonclassicality in communication networks, *Phys. Rev. A* **92**, 022351 (2015).
- [27] O. Rudolph, Further results on the cross norm criterion for separability, *Quantum Inf. Process.* **4**, 219 (2005).
- [28] K. Chen and L.-A. Wu, A matrix realignment method for recognizing entanglement, *Quantum Inf. Comput.* **3**, 193 (2003).
- [29] T. Moroder and O. Gittsovich, Calibration-robust entanglement detection beyond Bell inequalities, *Phys. Rev. A* **85**, 032301 (2012).
- [30] G. Sentís, J. N. Greiner, J. Shang, J. Siewert, and M. Kleinmann, Bound entangled states fit for robust experimental verification, *Quantum* **2**, 113 (2018).
- [31] R. F. Werner and M. M. Wolf, All-multipartite Bell-correlation inequalities for two dichotomic observables per site, *Phys. Rev. A* **64**, 032112 (2001).
- [32] Y.-C. Liang, C.-W. Lim, and D.-L. Deng, Reexamination of a multisetting Bell inequality for qudits, *Phys. Rev. A* **80**, 052116 (2009).
- [33] K. F. Pál and T. Vértesi, Maximal violation of a bipartite three-setting, two-outcome Bell inequality using infinite-dimensional quantum systems, *Phys. Rev. A* **82**, 022116 (2010).
- [34] A. Tavakoli, A. Pozas-Kerstjens, P. Brown, and M. Araújo, Semidefinite programming relaxations for quantum correlations, *Rev. Mod. Phys.* **96**, 045006 (2024).
- [35] K. Macieyszczak, M. Fraas, and R. Demkowicz-Dobrzański, Bayesian quantum frequency estimation in presence of collective dephasing, *New J. Phys.* **16**, 113002 (2014).
- [36] A. Tavakoli, M. Pawłowski, M. Żukowski, and M. Bourenane, Dimensional discontinuity in quantum communication complexity at dimension seven, *Phys. Rev. A* **95**, 020302 (2017).
- [37] R. A. da Silva and B. Marques, Semidefinite-programming-based optimization of quantum random access codes over noisy channels, *Phys. Rev. A* **107**, 042433 (2023).
- [38] M. Navascués and T. Vértesi, Activation of nonlocal quantum resources, *Phys. Rev. Lett.* **106**, 060403 (2011).
- [39] M. Navascués, E. Wolfe, D. Rosset, and A. Pozas-Kerstjens, Genuine network multipartite entanglement, *Phys. Rev. Lett.* **125**, 240505 (2020).
- [40] Á. Lukács, R. Trényi, T. Vértesi, and G. Tóth, Optimizing local Hamiltonians for the best metrological performance (2022), arXiv:2206.02820 [quant-ph].
- [41] G. Vidal and R. F. Werner, Computable measure of entanglement, *Phys. Rev. A* **65**, 032314 (2002).
- [42] M. L. Almeida, S. Pironio, J. Barrett, G. Tóth, and A. Acín, Noise robustness of the nonlocality of entangled quantum states, *Phys. Rev. Lett.* **99**, 040403 (2007).
- [43] R. F. Werner, Quantum states with Einstein-Podolsky-Rosen correlations admitting a hidden-variable model, *Phys. Rev. A* **40**, 4277 (1989).
- [44] C. Lancien, S. Di Martino, M. Huber, M. Piani, G. Adesso, and A. Winter, Should entanglement measures be monogamous or faithful?, *Phys. Rev. Lett.* **117**, 060501 (2016).

- [45] D. DiVincenzo, D. Leung, and B. Terhal, Quantum data hiding, *IEEE Transactions on Information Theory* **48**, 580 (2002).
- [46] P. Badziag, K. Horodecki, M. Horodecki, J. Jenkinson, and S. J. Szarek, Bound entangled states with extremal properties, *Phys. Rev. A* **90**, 012301 (2014).
- [47] A. C. Doherty, P. A. Parrilo, and F. M. Spedalieri, Distinguishing separable and entangled states, *Phys. Rev. Lett.* **88**, 187904 (2002).
- [48] N. Johnston, QETLAB: A MATLAB toolbox for quantum entanglement, version 0.9, <https://qetlab.com> (2016).
- [49] G. Tóth, QUBIT4MATLAB package, see the actual version at, <https://www.mathworks.com/matlabcentral/fileexchange/8433>.
- [50] F. Benatti, R. Floreanini, and M. Piani, Non-decomposable quantum dynamical semigroups and bound entangled states, *Open Syst. Inf. Dyn.* **11**, 325 (2004).
- [51] C. de Gois, K. Hansenne, and O. Gühne, Uncertainty relations from graph theory, *Phys. Rev. A* **107**, 062211 (2023).
- [52] J. Moerland, N. Wyderka, H. Kampermann, and D. Bruß, Bound entangled Bell diagonal states of unequal local dimensions, and their witnesses, *Phys. Rev. A* **109**, 012217 (2024).
- [53] H.-P. Breuer, Optimal entanglement criterion for mixed quantum states, *Phys. Rev. Lett.* **97**, 080501 (2006).
- [54] W. Hall, Constructions of indecomposable positive maps based on a new criterion for indecomposability (2006), arXiv:quant-ph/0607035 [quant-ph].